Ultrafast solvation dynamics explored by nonlinear optical spectroscopy

de Boeij, Wilhelmus Petrus ; Wiersma, D. A.

Chapter 1

Introduction

Chapter 1

Abstract

Chemical reaction dynamics and chemical rate processes in the liquid phase are strongly influenced by specific interactions between the solvent and the reactants. The study of solvation dynamics is aimed at a full characterization of the static as well as dynamic properties of the solute-solvent interaction. The dynamical interaction between the solute and the surrounding solvent causes fluctuations in the solute's electronic energy levels, which can be probed using various (non-)linear optical spectroscopic techniques. For the modelling of the coupling of the solute to the surrounding bath, the multimode Brownian oscillator model (MBO) is applied. In this model the energy gap fluctuations can be correlated to motions along a specific set of nuclear coordinates. The MBO model furthermore predicts the results for various (non-)linear spectroscopic experiments. In the last part of this introductory chapter, a short outline of the thesis is presented where the applied non-linear optical spectroscopic methods, based on the general concept of the time-domain four-wave mixing technique are discussed.

1.1 Molecular rate processes and solvation dynamics.

The dynamics of molecular rate processes in the liquid phase, is intimately connected to the process of solvation dynamics.[1-14] In fact, very often it is the action of the surrounding solvent that determines whether a reaction occurs or not. In some cases the solvent might act as a catalytic environment, lowering the reaction barrier, in other cases it can make this reaction-barrier higher. It might even be so that the solvent cage itself, after the chemical reaction-event, prevents the reaction species to escape the reaction area, resulting in geminate recombination.[15] A full understanding of chemical reactivity traces back to the basic understanding of the influence of the surrounding solvent on the electronic transition. Given the chemical and biological importance of various liquid state processes, much effort has thus been devoted, both theoretically as well as experimentally to the understanding of the process of solvation.[1-49]

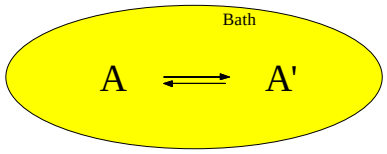

In the above diagram the unimolecular reaction from a species A to A′ is depicted, and takes place in the presence of a mediating bath. Among the unimolecular reactions, the electron transfer reactions[2,6-13,17] and photo-isomerization processes[1,11-13,18-20] are probably the most striking examples. Figure 1.1a depicts the typical potential surfaces applicable to the unimolecular reaction. For this ‘simple’ reaction mechanism, concepts such as reaction barrier, activation energies, forward and backward reaction rates as well as the coupling to the solvent should be closely considered. Note that only in the static regime a diagram as presented in Figure 1.1a can be applied. Solvent induced dynamical interactions with the reactants result in changes in the shape and position of the potential surfaces, thereby changing reaction parameters such as the energy gap. A detailed knowledge of the solvation processes, is thus of crucial importance to the understanding of molecular rate processes and chemical reaction dynamics in the liquid state. Over a complete range of time scales, the dynamical parameters of the solute-solvent interaction should be determined.

To study the effect of the mediating solvent, the problem is reduced to its simplest form. The reaction coordinate is excluded from the system and only the initial reactant will be used as a probe for solvation dynamics. A typical optical experiment that is sensitive to the solvation process is given in figure 1.1b, where the solvation upon electronic excitation is depicted. The system relaxes in the excited state potential as a result of the dissipative

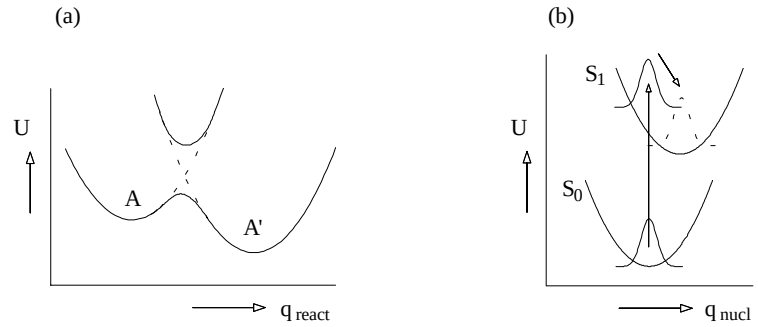

Fig. 1.1. (a) Potential energy surfaces (solid lines) for a unimolecular reaction scheme. A denotes the initial reactant whereas A′ denotes the product state. The reaction coordinate q_{react} is given along the x-axis of the graph. (b) Schematic diagram of the solvation process in the excited state. The potential surfaces for the ground state (S_0) and excited state (S_1) are depicted by solid lines. The optical excitation and subsequent relaxation along the nuclear coordinate are denoted by the arrows.

interaction with the surrounding bath.

The shape of the optical transition in the frequency domain, as observed in absorption spectroscopic measurements, represents the first observable of the system dynamics.[21-27] In liquids, the presence of broad and featureless bands complicates a direct and accurate band-shape analysis. In fact, the observation of a tremendous broadening in the optical lineshape of a dissolved molecule compared to the vacuum-state absorption lineshape is a direct indication of the strong interaction of the surrounding solvent on the optical transition of a probe molecule. The inability of the direct absorptive methods to distinguish between different dynamical processes (homogeneous and inhomogeneous), motivated the use of nonlinear spectroscopic methods.[28-49]

The developments in the generation of ultrafast laser-pulses, with pulse-durations close to the typical vibrational period of molecular vibrations,[50-53] have led to a situation that non-linear ultrafast spectroscopic measurements can now easily be conducted. In an optical experiment, a full knowledge of the transient induced polarization must be regarded as the optimum achievable goal. How this transient polarization depends on the various system parameters would be the full course of the experiment. Different linear and non-linear optical experiments provide the experimentalist with considerable insight in the dynamical and static properties of the optical transition dipole.

The dynamical properties of the solvation are captured in the time-dependent modulation of the molecular energy levels of the probe molecule.

$$\delta E_i(t) = E_i(t) - \langle E_i \rangle \tag{1.1}$$

where i labels the particular energy level (S_0, S_1, S_2,...). Given the macroscopic character of

the discussed problem, the ensemble average ($\langle..\rangle$) will be taken. The ensemble averaged energy level fluctuations can be expressed in the form of a time-dependent correlation function:

$$C_i(t) = \frac{\langle \delta E_i(0)\ \delta E_i(t)\rangle}{\langle \delta E_i^2\rangle} \tag{1.2}$$

Direct probing of the energy of a particular level ($E_i(t)$) by means of spectroscopic methods is not possible, rather the difference between two (or more) levels can be accurately monitored. The property $E_i(t)$ seems thus not a direct spectroscopic observable, but the energy difference between the electronic levels $\Delta E(t)$, where $\Delta E(t)=E_i(t)-E_j(t)$ is probed. The quantity $\Delta E(t)$ is the time-dependent transition frequency and is usually denoted as $\nu(t)$. In the form of a correlation function the fluctuations in the energy gap are given by:

$$C_{\Delta E}(t) = \frac{\langle \delta \Delta E(0)\ \delta \Delta E(t)\rangle}{\langle \delta \Delta E^2\rangle} = \frac{\langle \delta \nu(0)\ \delta \nu(t)\rangle}{\langle \delta \nu^2\rangle} \tag{1.3}$$

The measurement of the solvation dynamics as is captured in the correlation function C(t), is only sensitive to that part of the dynamics that is different in the electronic states. In other words, the experiment is sensitive to fluctuations in the energy gap ($\delta \Delta E(t)$) rather than sensitive to the fluctuation in a single energy level ($\delta E_i(t)$). The above correlation function $C_{\Delta E}(t)$ can be obtained from various optical experiments.

1.2 Optical spectroscopy

Figure 1.2 depicts the layout of a general optical experiment. Three major units can be distinguished, the light source, the sample, and the detector. The light source provides the experimentalist with the necessary (shaped and well-characterized) optical radiation. After having excited the optically active sample in a particular way, a scala of detection methods can be applied to monitor any optically induced signal. Different experiments can be conducted to unravel sample-parameters and sample-parameter-dependencies by proper selection of the specific excitation conditions, sample conditions and detection characteristics.

Fig. 1.2. General layout of an optical spectroscopic experiment. The three different element in the experiment, the excitation source, the optically active sample and the detection method are represented by boxes. In between the boxes, the excitation and signal fields are given by the arrows.

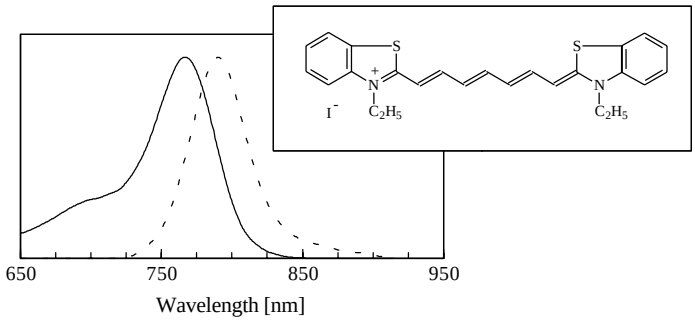

Fig. 1.3. Linear absorption spectrum (solid line) and steady state emission spectrum (dashed line) of the IR-dye molecule DTTCI dissolved in ethylene glycol. The inset depicts the molecular structure of DTTCI (3,3'-diethylthiatricarbocyanine iodide).

Optical spectroscopic techniques differ in the characteristics of the excitation fields applied to the sample. Generally two classes can be defined, the time-domain and the frequency-domain spectroscopy. In the time-domain experiments the temporal duration of the excitation pulse can be regarded as short on the timescale of the dynamics of the system. Spectrally this is equivalent to the condition that the spectrum of the excitation source exceeds the linewidth of the relevant optical transition. The selectivity of probing the dynamics in the time domain, relaxes the particular sensitivity in the spectral domain. Different classes of time-domain experiments such as pump-probe,[28,29] photon echo, [30-37]transient grating scattering,[38] time-gated fluorescence,[40-43] and transient absorption spectroscopy[44-46] have been used to investigate the problem of solvation dynamics.

The frequency domain experiments distinguish themselves by their selectivity in the frequency domain. Inherently to the spectral sensitivity, temporal resolution is relaxed. Also in the frequency domain, techniques such as resonance light scattering,[47] two-colour picosecond CARS,[48,49] and absorption/emission spectroscopy[54] have been applied as probes of solvation dynamics as well.

Time-domain and the frequency-domain spectroscopies are complementary in terms of their sensitivity with respect to certain time scales and it is therefore essential to consider both domains in order to acquire a complete picture of solvent motion. While Fourier-transform relations exist both for linear and nonlinear optical susceptibilities,[55] time-domain optical experiments have the possibility of creating a time-window through which molecular motion can be explored.[56] In this thesis we address various time domain non-linear optical methods, to unravel the optical dynamics of solvation.

1.3 Optical probe and light-matter interaction

The probe molecule used in the study of solvation dynamics, is the infrared dye molecule DTTCI (3,3'-diethylthiatricarbocyanine iodide).[57] Figure 1.3 depicts the absorption spectrum and steady-state fluorescence spectrum of this molecule when dissolved in ethylene glycol. The absorption and emission spectrum of the dissolved probe are characterized by broad and structureless bands. When performing an optical experiment on this dissolved system, the interaction of the sample with the incident fields introduces a time-dependent material polarization P(**r**,t). Maxwell's equations furthermore describe the generation and propagation of an optical signal field, E_s(**r**,t) in the presence of the material polarization P(**r**,t).

For a description of a non-linear spectroscopic experiment, a perturbative expansion of the density matrix evolution is used, as is discussed in numerous textbooks.[58,59] The reduced density matrix description allows for a concise description of the complicated multi-particle system. A full characterization of the systems density matrix provides a complete picture of any ensemble averaged observable. The time-evolution of the density matrix elements is dictated by the Liouville equation. By applying a perturbative evaluation of the Liouville equation, the system evolution can be captured in a set of response functions. In general these response functions are multiple-point dipole correlation functions, but can by means of a (second order) cumulant expansion be reduced to a specific sequence of two-point correlation functions, that can be expressed in the energy gap correlation function C(t) (Eq.(1.3)).

To characterize the specific time-dependent properties of the energy gap, we will now address the modelling of the system and the system-bath interaction. The presence of a significant number of surrounding and interacting solvent molecules constitutes a large number of multi-particle interactions. A fully quantum-mechanical approach is thus in view of the large number of degrees of freedom beyond any realistic goal. One has to rely on some reduced description.[16] In this thesis we will make use of the multimode Brownian oscillator (MBO) model or spin-boson Hamiltonian for a phenomenological description of molecular motions in liquids.[60-64] In the MBO model, the system Hamiltonian is dressed by a set of harmonic nuclear oscillators that are subsequently harmonically coupled to a set of bath coordinates. The total Hamiltonian of the coupled system can be separated in three parts:

$$H_T = H + H' - \mu \cdot E(t) \tag{1.4}$$

where H represents the system Hamiltonian, H′ the coupling to the bath and μE(t) the coupling to the electromagnetic field. The uncoupled system Hamiltonian H is given by:

$$H = |g\rangle H_g \langle g| + |e\rangle H_e \langle e| \tag{1.5}$$

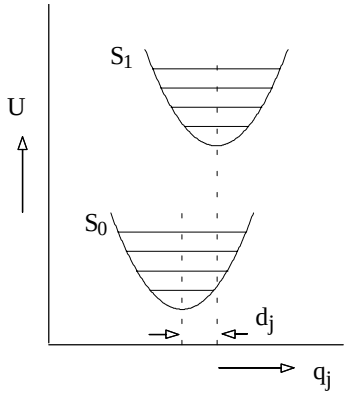

Fig. 1.4. The molecular ground (S_0) and excited (S_1) potential energy surfaces as applied in the MBO model. Both electronic levels (S_0 and S_1) are dressed by a harmonic nuclear mode. The potentials are displaced along the nuclear q_j-coordinate by an amount d_j.

and the coupling to the electromagnetic field is expressed as:

$$\mu = |e\rangle \mu_{eg} \langle g| + |g\rangle \mu_{ge} \langle e| \tag{1.6}$$

In modelling the ground state and excited state Hamiltonian we assume both potentials to be harmonic. The excited state potential surface is displaced along the nuclear coordinate q_j by an amount d_j (Figure 1.4) Within this harmonic approach the q_j-dependence of the electronic energy gap (U) is thus defined as:

$$U = \sum_j m_j \omega_j^2 d_j q_j \tag{1.7}$$

and constitutes a direct relation between the electronic energy gap U, and the quantum-mechanical nuclear coordinates q_j. Any change or fluctuation in the nuclear coordinate q_j is (linearly) reflected in a change in the electronic energy gap.

For the modelling of the bath modes (H' in Eq.(1.7)), a second series of harmonic oscillators (bosonic bath) is taken, that is coupled to the nuclear harmonic coordinates. In figure 1.5 the hierarchy of the system-bath interaction model is depicted. Three levels can be distinguished in the hierarchy, the optical two level system, the nuclear coordinates and the bath modes. In the Ohmic dissipation limit, the distribution of the bath oscillators coupled to the system is assumed to be a uniform. In this case a single frequency independent damping constant $\gamma_j(\omega)=\gamma_j$ characterizes the nuclear mode and direct analytical relations can be derived for the time-domain energy gap correlation functions C(t).[59]

Having captured the dynamics of solvation, and thus the interaction of the solvent on the dissolved solute, we are now in the position to readdress the unimolecular reaction scheme. For instance, it has long been recognized that electron transfer reactions are usually controlled

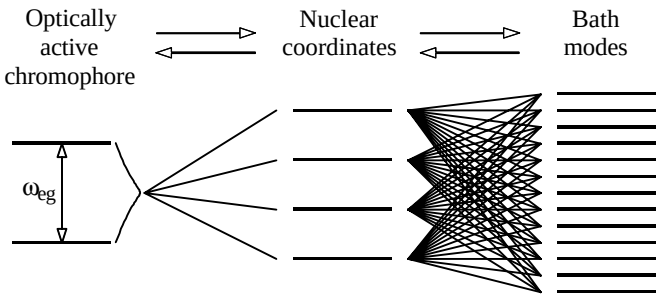

Fig. 1.5. Schematic hierarchy of the system bath modeling

by the dynamics of dielectric fluctuations in the surrounding medium (the solvent). Favourable fluctuations, which make the initial and final state temporarily isoenergetic, are crucial in inducing the electron transfer. In the Marcus theory these fluctuations are treated through a classical dielectric continuum formulation.[10]

Similar as for the Marcus theory, the MBO model provides a route to retrieve the chemical reaction rate (electron transfer) for this class of reaction processes.[2,17,61] The coupling between the two states is explicitly included in the system Hamiltonian, and is expressed with the following relation:

$$H = |g\rangle H_g \langle g| + |e\rangle H_e \langle e| + V\left(|g\rangle\langle e| + |e\rangle\langle g|\right) \tag{1.8}$$

where V presents the coupling between the two reacting species. Within a harmonic approximation, relations for the reaction rates can be deduced that include the absorption lineshape function as well as a specific solvent time-scale function.[2,17] The specific nature of the solvent-induced fluctuations is included in this solvent time-scale function. With the results from various non-linear optical experiments a correlation function can be established that characterizes the fluctuations in the electronic energy gap. This furthermore determines the solvent time-scale function and allows the prediction of electron transfer rates. Similar to the electron transfer system, the same approach can be applied for photo-isomerization reactions.

1.4 Outline of the thesis

In Chapter 2 we address the design of the light source that is used as the excitation source in the time-domain non-linear experiments. The laser is based on the short pulse cw-mode-locked Ti:sapphire laser and extended by incorporation of a cavity-dumper section. The major virtue of this laser is that it combines the excellent optical properties of the radiation one normally obtains from a cw-mode-locked femtosecond Ti:sapphire laser with the merits of

the process of cavity-dumping, namely a reduced repetition rate and an enhanced pulse energy. Near 10-fs pulse durations, variable repetition rates and increased (with respect to the cw-mode-locked laser) pulse energies, in combination with excellent stability and system durability make this laser an attractive source that can directly be used for non-linear optical experiments. In the remaining part of the thesis several non-linear time-domain spectroscopic methods will be applied as tools in the study of the solvation dynamics.

Chapter 3 reports on the time-integrated and time-resolved time domain four-wave mixing experiment. Figure 1.6a depicts the layout of the conventional experimental configuration for the stimulated photon echo. Three short optical pulses excite the sample and a signal is generated in the phase-matched direction. In the depicted configuration, a time-integrated detector monitors the total emitted signal power. In Chapter 3 the so-called photon echo peak shift method is introduced, enabling the experimentalist to determine a first-order approximation of the system-bath correlation function. The conventional time-integrated stimulated photon echo is extended by time-resolving the emitted polarization on a femtosecond time scale. This method provides further inside in the short time dynamics of the system bath correlation function. Figure 1.6b shows the configuration of the time-gate that operates through a non-linear interaction of the signal beam with a short optical gate pulse. In the same chapter, the theoretical description of the system-bath interaction based on the spin-boson Hamiltonian formalism is presented. This formalism is applied as a model for the interaction between solute and solvent, and is used to fit the experimental results. Based on linear and non-linear spectroscopic experiments, a correlation function is derived that within the MBO model can describe all measured data.

Although the time-gated detection (Chapter 3) reveals some of the temporal

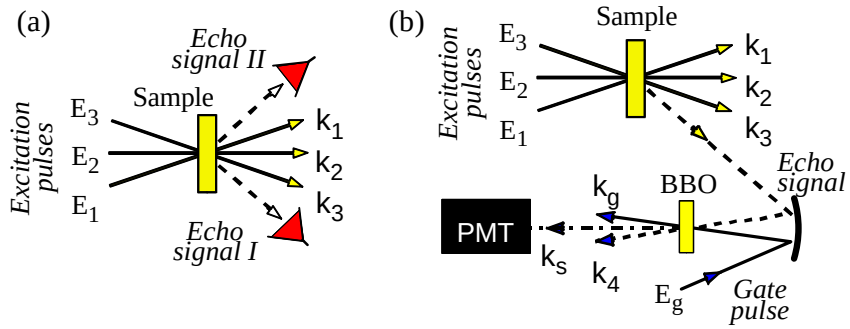

Fig. 1.6. (a) Layout of the time-integrated stimulated photon echo experiment. Three pulses excite that sample and the coherent signal is detected in the phase-matched direction. The time resolution of the applied intensity detector is insufficient to resolve the signal, and thus monitors the total integrated signal intensity. (b) Stimulated photon echo experiment equipped with a time-gate, based on the non-linear upconversion method. The transient signal is mixed externally in a non-linear upconversion crystal with the short optical gate pulse and the resulting second harmonic signal is monitored.

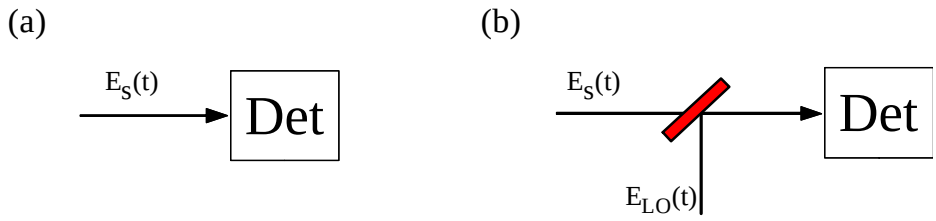

Fig. 1.7. (a) Homodyne detection method. The signal is detected in the background-free direction by a quadratic detector (Det). (b) Heterodyne detection method. The signal is interferometrically mixed with a local oscillator field, and directed to the detector (Det).

characteristics of the transient echo signal, the measured profile only relates to the signal amplitude. Any (temporal) phase information on the transient polarization is lost. To access the temporal phase of the transient signal, interferometric detection methods such as the heterodyning of the signal can be applied.

Figure 1.7 depicts two methods of signal detection. In panel (a) the homodyne detection method is given. A signal emitted in a background-free direction is recorded by a quadratic detector. Depending on the speed of the detector, a time-integrating signal (slow detector) or time-resolved (fast detector) is recorded. In the panel (b), the heterodyne detection method is given. Here, the optical signal field is interferometrically mixed with a local oscillator field and the sum of the two is directed to the intensity detector. In the heterodyne configuration, the temporal resolution can be acquired using a local oscillator in the form of a short optical pulse. Changing the phase of the local oscillator with respect to the signal field, allows the determination of the in-phase and in-quadrature components of the emitted signal, and provides information on the real and imaginary components of the signal. In other words, both amplitude and phase of the transient signal can be time-resolved.

In Chapter 4, the results of the heterodyne detection of the stimulated photon echo (HSPE) will be presented. A theoretical base of the heterodyne detection of the echo is presented and the multimode Brownian oscillator description is included in the signal description. The concept of phase-locked femtosecond laser pulses is given and applied to the heterodyne detection of the echo. The technique is applied as a tool to investigate the dynamics of solvation in the liquid phase. Experiments are reported on the infrared dye molecule DTTCI in the solvent ethylene glycol. From the HSPE measurements the instantaneous amplitude and frequency of the emitted (non-linear polarization induced) signal can be derived. Changes in the frequency directly relate to the dynamical Stokes shift and the energy reorganization process in the solute-solvent system. The experimental results are successfully fitted to the multimode Brownian oscillator model, and corroborate the results as measured by the conventional time-gated echo technique, as reported in Chapter 3.

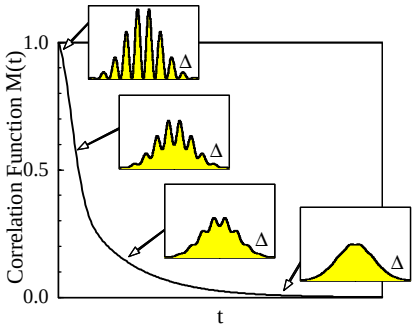

Fig. 1.8. System bath correlation function as a function of time (t). At four different values of the correlation function the shape of the induced frequency grating is schematically depicted (insets). Δ is the frequency coordinate.

As can be inferred from the molecular structure depicted in figure 1.3(inset), the probe molecule contains a significant number of internal vibrational degrees of freedom. Although in general only a specific set of these modes is (strongly) coupled to the electronic transition, these coupled modes can affect the observed optical transients. For those studies which are aimed at a better understanding of the solute-solvent interaction, the presence of these intramolecular modes hampers the direct interpretation of the observed decays. Suppression of these modes would be quite valuable in studying the problem of solvation dynamics. In Chapter 5 we present the successful application of phase-locked laser pulses towards the method of vibrational mode-suppression. The method is experimentally demonstrated and accomplished by means of femtosecond phase-locked heterodyne detection of the stimulated photon echo.

In Chapter 6 the properties of the transient nonlinear optical signal are explored in the frequency domain. As the experimental arrangement, the phase-locked pump-probe (PLPP) configuration is used, where two pulses induce a frequency grating [65] and a third pulse acts as the probe pulse. Based on the concept of frequency gratings, the solute-solvent interaction is studied. Stochastic modulation of the transition frequency causes the induced frequency grating to blur in time. This effect is schematically demonstrated in figure 1.8. Depending on the value of the correlation function at the time of the probing pulse, the induced grating exhibits a specific contour. As time progresses and the correlation function decays, the induced modulation features in the spectrum disappear. In Chapter 6 these induced spectral interferences are monitored for different probing times. Results of the frequency-resolved PLPP experiment are presented and are compared to calculations based on the MBO model.

In Chapter 7 we address the concept of Liouville pathways interference. For the experimental demonstration of this effect we use the HSPE experiment, which was previously presented in Chapter 4. The constructive and destructive interferences in time-domain spectroscopy are demonstrated for third-order signals. Higher intensities applied to the sample

result in the generation of fifth-order signal that contribute to the final signal. It is shown that interferences can also be monitored between the third-order and fifth-order signals. Under specific conditions a situation can occur that the complete signal disappears as a result of a full destructive interference. The technique both in a low intensity limit (third-order signal) as well as in a high intensity limit (up to fifth-order signals) present an example of an optical control experiment through Liouville pathway interference. The control over the generated signal is exercised by manipulation of the phases of the incident pulses.

References

1. G.A. Voth, R.M. Hochstrasser, J. Phys. Chem. **100**, 13034 (1996) and references therein.
2. S. Mukamel, Y.J. Yan, Acc. Chem. Res. **22**, 301, (1989) and references therein; J. Phys. Chem. **60**, (1986) special issue.
3. H.A. Kramers, Physica **7**, 284 (1940).
4. R.F. Grote, J.T. Hynes, J. Chem. Phys. **73**, 2715 (1980); *ibid.* **74**, 4465 (1981).
5. P. Hänggi, P. Talkner, M. Borkovec, Rev. Mod. Phys. **62**, 250 (1990).
6. M.W. Makinen, S.A. Schichman, S.C. Hill, H.B. Gray, Science **222**, 929 (1983).
7. G.L. Closs, J.R. Miller, Science **240**, 440 (1988).
8. G. McLendon, Acc. Chem. Res. **21**, 160 (1988).
9. E.M. Kosower, D. Huppert, Annu. Rev. Phys. Chem. **37**, 127 (1986).
10. R.A. Marcus, N. Sutin, Biochem. Biophys. Acta **811**, 275 (1985); H. Sumi, R.A. Marcus, J. Chem. Phys. **84**, 4894 (1986).
11. P.F. Barbara, W. Jarzeba, Acc. Chem. Res. **21**, 195 (1988).
12. G.R. Fleming, *Chemical Applications of Ultrafast Spectroscopy* (Oxford University Press, 1986); *Femtosecond Reaction Dynamics*; edited by D.A. Wiersma (North Holland, Amsterdam, 1994); *Femtochemistry: Ultrafast dynamics of the chemical bond*; edited by A.H. Zewail (World Scientific, Singapore, 1994).
13. J.T. Hynes, Ann. Rev. Phys. Chem. **36**, 573 (1985); G.R. Fleming, P.G. Wolynes, Physics Today **43**, 36 (1990); J.D. Simon, Acc. Chem. Res. **21**, 128 (1988); P.F. Barbara, W. Jarzeba, Adv. Photochem. **15**, 1 (1990); P.J. Rossky, J.D. Simon, Nature **370**, 263 (1994).
14. G. van der Zwan, J.T. Hynes, J. Phys. Chem. **89**, 4181 (1985); M. Maroncelli, J. Chem. Phys. **94**, 2084 (1991); *ibid.* J. Mol Liq. **57**, 1 (1993); M. Maroncelli, G.R. Fleming, J. Chem. Phys. **89**, 5044 (1988); E.A. Carter, J.T Hynes, J. Chem. Phys. **94**, 5961 (1991); L. Perera, M.L. Berkowitz, J. Chem. Phys. **96**, 3092 (1992); *ibid*. **97**, 5253 (1992); E. Neria, A. Nitzan, J. Chem. Phys. **96**, 5433 (1992); M. Maroncelli, P.V. Kumar, A. Papazyan, J. Phys. Chem. **97**, 13 (1993); S. Roy, S. Komath, B. Bagchi, J. Chem. Phys. **99**, 3139 (1993); S. Roy, B. Bagchi, J. Chem. Phys. **99**, 9938 (1993); R.M. Stratt, M. Cho, J. Chem. Phys. **100**, 6700 (1994); B.M. Ladanyi, R.M. Stratt, J. Phys. Chem. **99**, 2502 (1995); P.V. Kumar, M. Maroncelli, J. Chem. Phys. **103**, 3038 (1995).
15. J. Franck, E. Rabinowitch, Trans. Faraday Soc. **30**, 120 (1934).
16. For an overview of different reduced descriptive models see: E.J.T. Nibbering, thesis University Groningen, The Netherlands, (1993) chapter 2; E.T.J. Nibbering, D.A. Wiersma, K. Duppen, Chem. Phys. **183**, 167 (1994); L.E. Fried, N Bernstein, S. Mukamel, Phys. Rev. Lett. **68**, 1842 (1992); N.E. Shemetulskis, R.F. Loring, J. Chem. Phys. **97**, 1217 (1992).
17. S. Mukamel, Adv. Chem. Phys. **70**, Part I, 165 (1988); S. Mukamel, R.F. Loring, J. Opt. Soc. Am. B **3**, 595 (1986); Y.J. Yan, S. Mukamel, J. Chem. Phys. **89**, 6160 (1988); R.F. Loring, Y.J. Yan, S. Mukamel, J. Chem. Phys. **87**, 5840 (1987); M. Sparpaglione, S. Mukamel, J. Chem. Phys. **88**, 3263 (1988); *ibid.* J. Chem. Phys. **88**, 4300 (1988); Y.J. Yan, M. Spargaglione, S. Mukamel, J. Phys. Chem. **92**, 4842 (1988).

18. R.M. Hochstrasser, Pure Appl. Chem. **52**, 2683 (1980); R.M. Hochstrasser, R.B. Weisman, In *Radiationless Transitions;* edited by S.H. Lin, (Academic Press: New York, 1982).
19. D.H. Waldeck, Chem. Rev. **91**, 415 (1991) and references therein.
20. *Activated Barrier Crossing;* edited by G.R. Fleming, P. Hänggi, (World Scientific: Singapore, 1993).
21. Y. Yan, K. Nelson, J. Chem. Phys. **87**, 6240 (1987); *ibid.* J. Chem. Phys. **87**, 6257 (1987); Y.J. Yan, L.T. Cheng, K. Nelson, *Advances in Nonlinear Spectroscopy;* edited by R.J.H. Clark, R.E. Hester, (Wiley: New York, 1988). D. McMorrow, W.T. Lotshaw, G.A. Kenney-Wallace, IEEE J. Quantum Electron. QE-**24**, 443 (1988).
22. M.J. Rosker, F.W. Wise, C.L. Tang, Phys. Rev. Lett. **57**, 321 (1986); I.A. Walmsley, M. Mitsunaga, C.L. Tang, Phys. Rev. A **38**, 4681 (1988).
23. M. Maroncelli, G.R. Fleming, J. Chem. Phys. **89**, 875 (1988); *ibid.* J. Chem. Phys. **86**, 6221 (1987).
24. R.A. Mathies, C.H. Brito Cruz, W.T. Pollard, C.V. Shank, Science **240**, 777 (1988).
25. J. Chesnoy, A. Mokhtari, Phys. Rev. A **38**, 3566 (1988); S. Saikan, Phys. Rev. A **38**, 4669 (1988).
26. A.H. Zewail, R.B. Bernstein, Chem. Eng. News **66**, 24 (1988).
27. S. Mukamel, Phys. Rev. A **28**, 3480 (1983). R.W. Boyd, S. Mukamel, *ibid*. **29**, 1973 (1984).
28. P. Cong, H. Deuel, J.D. Simon, Chem. Phys. Lett. **212**, 367 (1993); *ibid.* J. Chem. Phys. **100**, 7855 (1994).
29. H.L. Fragnito, J.-Y. Bigot, P.C. Becker, C.V. Shank, Chem. Phys. Lett. **160**, 101 (1989); W.T. Pollard, S.-Y. Lee, M.A. Mathies, J. Chem. Phys. **7**, 4012 (1992); C.J. Bardeen, Q. Wang, C.V. Shank, Phys. Rev. Lett. **75**, 3410 (1995).
30. P.C. Becker, H.L. Fragnito, J.-Y Bigot, C.H. Brito Cruz, R.L. Fork, C.V. Shank, Phys. Rev.Lett. **63**, 505 (1989); W.T. Pollard, H.L. Fragnito, J.-Y Bigot, C.V. Shank, R.A. Mathies, Chem. Phys. Lett. **168**, 239 (1990); J.-Y Bigot, M.T. Portella, R.W. Schoenlein, C.J. Bardeen, A. Migus, C.V. Shank, Phys. Rev. Lett. **66**, 1138 (1991); C.J. Bardeen, C.V. Shank, Chem. Phys. Lett. **226**, 310 (1994).
31. E.T.J. Nibbering, D.A. Wiersma, K. Duppen, Phys. Rev. Lett. **66**, 2464 (1991); E.T.J. Nibbering, D.A. Wiersma, K. Duppen, J. Photochem. Photobiol. A **62**, 347 (1992); K. Duppen, F. de Haan, E.T.J. Nibbering, D.A. Wiersma, Phys. Rev. A **47**, 5120 (1993); E.T.J. Nibbering, D.A. Wiersma, K. Duppen, Chem. Phys. **183**, 167 (1994); K. Duppen, E.T.J. Nibbering, D.A. Wiersma, in *Femtosecond Reaction Dynamics*, edited by D.A. Wiersma, (North Holland, Amsterdam, 1994), pp. 197-208.
32. R. Zhang, T.-S. Yang, A.B. Myers, Chem. Phys. Lett. **112**, 541. (1993).
33. T. Joo, A.C. Albrecht, Chem. Phys. **176**, 233 (1993).
34. W.P. de Boeij, M.S. Pshenichnikov, K. Duppen, D.A. Wiersma, Chem. Phys. Lett. **224**, 243 (1994); W.P. de Boeij, M.S. Pshenichnikov, D.A. Wiersma, Chem. Phys. Lett. **238**, 1 (1995); M.S. Pshenichnikov, K. Duppen, D.A. Wiersma, Phys. Rev. Lett. **74**, 674 (1995).
35. S.J. Rosenthal, B.J. Schwartz, P.J. Rossky, Chem. Phys. Lett. **229**, 443 (1994).

36. M. Cho, G.R. Fleming, J. Chem. Phys. **98**, 3478 (1994); T. Joo, Y. Jia, G.R. Fleming, J. Phys. Chem. **102**, 4063 (1995); T. Joo, Y. Jia, J.-Y. Yu, M.J. Lang, G.R. Fleming, J. Chem. Phys. **104**, 6089 (1996); M. Cho, J.-Y. Yu, T. Joo, Y. Nagasawa, S.A. Pasino, G.R. Fleming, J. Phys. Chem. **100**, 11944 (1996); G.R. Fleming, M. Cho, Annu. Rev. Phys. Chem. **47**, 109 (1996).
37. P. Vöhringer, D.C. Arnett, R.A. Westervelt, M.J. Feldstein, N.F. Scherer, J. Chem. Phys. **102**, 4027 (1995); T.-S. Yang, P. Vöhringer, D.C. Arnett, N.F. Scherer, J. Chem. Phys. **103**, 8346 (1995); P. Vöhringer, D.C. Arnett, T.-S. Yang, N.F. Scherer, Chem.Phys.Lett. **237**, 387 (1995).
38. B.D. Fainberg, Isr. J. of Chem. **33**, 225 (1993).
39. A. Mokhtari, J. Chesnoy, A. Laubereau, Chem. Phys. Lett. **155**, 593 (1989); A. Mokhtari, A. Chebira, J. Chesnoy, J. Opt. Soc. Am. B **7**, 1551 (1990).
40. P.F. Barbara, G.C. Walker, T.P. Smith, Science **256**, 975 (1992).
41. S.J. Rosenthal, X. Xie, M. Du, G.R. Fleming, J. Chem. Phys. **95**, 4715 (1991); M. Cho, S.J. Rosenthal, N.F. Scherer, L.D. Ziegler, G.R. Fleming, J. Chem. Phys. **96**, 5033 (1992); S.J. Rosenthal, R. Jimenez, G.R. Fleming, P.V. Kumar, M. Maroncelli, J. Mol. Liq. **60**, 25 (1994); R. Jimenez, G.R. Fleming, P.V. Kumar, M. Maroncelli, Nature **369**, 471 (1994).
42. M.L. Horng, J. Gardecki, A. Papazyan, M. Maroncelli, J. Phys. Chem. **99**, 17311 (1995).
43. T. Gustavsson, G. Baldacchino, J.-C. Mialocq, S. Pommeret, Chem. Phys. Lett. **236**, 587 (1995).
44. W. Vogel, D.-G. Welsch, B. Wilhelmi, Phys. Rev. A **37**, 3825 (1988); W. Vogel, D.-G. Welsch, B. Wilhelmi, Chem. Phys. Lett. **153**, 376 (1988).
45. P.C. Becker, R.L. Fork, C.H. Brito Cruz, J.P. Gordon, C.V. Shank, Phys. Rev. Lett. **60**, 2462 (1988); C.H. Brito Cruz, R.L. Fork, W.H. Knox, C.V. Shank, Chem. Phys. Lett. **132**, 341 (1986).
46. D. Bingemann, N.P. Ernsting, J. Chem. Phys. **102**, 2691 (1995).
47. S.Y. Goldberg, E. Bart, A. Meltsin, B.D. Fainberg, D. Huppert, Chem. Phys. **183**, 217 (1994); B.D. Fainberg, Phys. Rev A. **48**, 849 (1993).
48. T. Yajima, Y. Taira, J. Phys. Soc. Jap. **47**, 1620 (1979).
49. B.A. Grishanin, V.M. Petnikova, V.V. Shuvalov, Zh. Prikl. Spektrosk. **47**, 966 (1987); *ibid.* **47**, 1002 (1987).
50. Springer Series in Chemical Physics, *Picosecond Phenomena* (Springer Verlag Berlin) Issue I(1978), II(1980), III(1982), and IV(1984); Springer Series in Chemical Physics, *Ultrafast Phenomena* (Springer Verlag Berlin) Issue V(1986), VI(1988), VII(1990), VIII(1992), IX(1994), and X(1996).
51. J.D. Simon, Rev. Sci. Instrum. **60**, 3597 (1989).
52. J.A. Valdmanis, R.L. Fork, J.P. Gordon, Opt. Lett. **20**, 3483 (1985); J.A. Valdamis, R.L. Fork, IEEE J. Quant. Electron. **22**, 112 (1986); R.L. Fork, C.H. Brito Cruz, P.C. Becker, C.V. Shank, Opt. Lett. **12**, 483 (1987).
53. M. T. Asaki, C. P. Huang, D. Garvey, J. Zhou, H. C. Kapteyn, M. M. Murnane, Opt. Lett. **18**, 977 (1993); Ch. Spielmann, P. F. Curley, T. Brabec, and F. Krausz, IEEE J. Quant. El., **30**, 1100 (1994); M.S. Pshenichnikov, W.P. de Boeij, D.A. Wiersma, Opt. Lett. **19**, 572 (1994).

54. E.T.J. Nibbering, D.A. Wiersma, K. Duppen, J. Chem. Phys. **93**, 5477 (1990).
55. For experimental verification of the transform relationship between Raman spectoscopies, see: S. Kinoshita, Y. Kai, M. Yamaguchi, T. Yagi, Phys. Rev. Lett. **75**, 148 (1995); S. Kinoshita, Y. Kai, M. Yamaguchi, T. Yagi, Chem. Phys Lett. **236**, 259 (1995); P. Cong, J.D. Simon, C.Y. She, J. Chem. Phys. **104**, 962 (1996).
56. Y.J. Yan, L.E. Fried, S. Mukamel, J. Phys. Chem. **93**, 8149 (1989).
57. The choice of this molecule is based on the fact that its absorption spectrum largely overlaps with the laser output spectrum. Contrary to other tested carbocyanine molecules, the two-pulse echo signal exhibits a significant asymmetry and a tail on the long-delay side. Furthermore the third order non-linear signal from this molecule is relative insensitive to higher order signal distortions upon increase of the intensity of the incident pulses. This point is further addressed in Chapter 2.
58. P.N. Butcher, D. Cotter, '*The elements of non-linear optics*', '*Cambridge studies in modern optics*', Vol 9, edited by P.L. Knight and W.J. Firth, (Cambridge University press, Cambridge, 1995).
59. S. Mukamel, *Principles of nonlinear optical spectroscopy*; (Oxford University Press, New-York, 1995).
60. M. Aihara, Phys. Rev. B **25**, 53 (1982).
61. Y.J. Yan, M. Sparpaglione, S. Mukamel, J. Phys. Chem. **92**, 4842 (1988); S. Mukamel, Y.J. Yan, Acc. Chem. Res. **22**, 310 (1989); Y.J. Yan, S. Mukamel, J. Chem. Phys. **89**, 5160 (1988); *ibid*, Phys. Rev. A **41**, 6485 (1990); *ibid*, J. Chem. Phys. **94**, 179 (1991); S. Mukamel, Adv. Chem. Phys. **70**(I), 165 (1988); *ibid.* Annu. Rev. Phys. Chem. **41**, 647 (1990); M. Cho, N.F. Scherer, G.R. Fleming, S. Mukamel, J. Chem. Phys. **96**, 5618 (1992); L.E. Fried, N. Bernstein, S. Mukamel, Phys. Rev. Lett. **68**, 1842 (1992); Y. Tanimura, S. Mukamel, Phys. Rev. E **47**, 118 (1993).
62. A.O. Caldiera, A.J. Leggett, Physic. A **121**, 587 (1983).
63. H. Grabert, P. Schramm, G.L. Ingold, Phys. Rep. **168**, 115 (1988).
64. Y. Gu, A. Widom, P.M. Champion, J. Chem. Phys. **100**, 2547 (1994).
65. K. Duppen, D.A. Wiersma, J. Opt. Soc. Am. B **3**, 614 (1986); K. Duppen, D.A. Wiersma, Science **237**, 1147 (1987); E.T.J. Nibbering, thesis University Groningen (1993) Chapter 8.